Eleventh International Conference on CFD in the Minerals and Process Industries
CSIRO, Melbourne, Australia
7-9 December 2015

MODELLING MIXING IN LANCE STIRRED REACTORS

Jan Erik OLSEN*, Mihaela POPESCU, Pål TETLIE

SINTEF Materials & Chemistry, 7465 Trondheim, NORWAY
*Corresponding author, E-mail address: Jan.E.Olsen@sintef.no

ABSTRACT

An Eulerian-Lagrangian modelling concept was developed to study mixing in gas stirred reactors where the gas is injected through a submerged lance. In order to validate the model, experiments in a 500 x 500 x 50 mm bath were conducted. In these experiments gas rates and positioning of the lance were varied. The model was compared to experimental velocity profiles and mixing characteristics. Both model results and experiments show that mixing increases with increasing gas rates, and by lowering the lance further into the bath. The model results are consistent with the experimental results.

NOMENCLATURE

d	diameter [m]
C	coefficient [ ]
F	force per mass [N/kg]
g	coefficient of gravity [m/s^2]
k	turbulent kinetic energy [m^2/s^2]
p	pressure [Pa]
U	average velocity [m/s]
u	velocity [m/s]
$ú$	velocity fluctuations [m/s]
Re	Reynolds number [ ]
t	time [s]
ϵ	turbulent dissipation rate [m^2/s^3]
ξ	random number
μ	dynamic viscosity [Pa s]
ρ	density [kg/m^3]
τ	eddy lifetime [s]

Indexes

b	bubble
eff	effective
D	drag
VM	virtual mass

INTRODUCTION

By blowing gas through lances submerged in liquid baths, mixing and interface reactions can be promoted. The technique is applied in many industrial reactors. In order to assess and optimize such processes, analysis by CFD can be performed. Different CFD approaches can be applied. Regardless of modelling approach, the model needs to capture the relevant physics. This includes conservation of mass and momentum, interactions between phases and turbulence.

An Eulerian-Lagrangian modelling concept has previously been demonstrated to accurately reproduce experimental results from gas liquid reactors with bottom injection of gas (Cloete *et al.*, 2009; Olsen & Cloete, 2009). The Eulerian-Lagrangian modelling concept is based on a VOF model for capturing the flow in the continuous phases and the interface between the continuous phases, and a discrete phase model, DPM, for tracking the bubble motion. Here the model is applied to gas-liquid reactors with gas injection through submerged lances.

In order to assure that the model provides reliable results, the model has been compared against experimental results. These results were obtained from a lab-scale reactor with air and water. Validation experiments and modelling were performed using a 800 x 500 x 50 mm vessel as seen in Figure 1. Water was filled up to a depth of 500 mm leaving 300 mm clearance on top. Gas was injected through a lance as illustrated.

In the following chapter the modelling concept is presented. Thereafter the experimental study is described before comparison of the model with respect to the experiments is shown. In the end some conclusions are extracted.

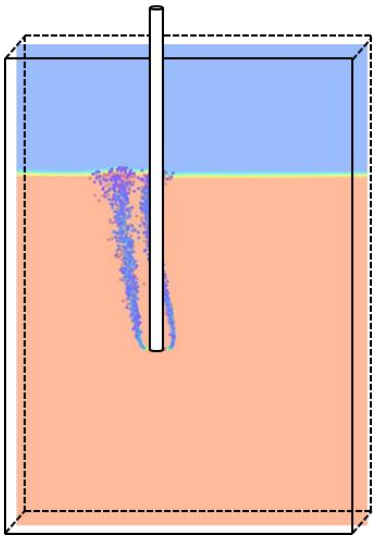

Figure 1: Vessel for experimental and numerical study.

MODEL DESCRIPTION

The hydrodynamic part of a bubble reactor model calculates the flow of bubbles, liquids and if necessary gas above liquids. In a Lagrangian framework the bubbles move according to Newton's second law. The bubble acceleration is given by a force balance:

$$\frac{d\boldsymbol{u}_b}{dt} = \frac{\boldsymbol{g}(\rho_b - \rho)}{\rho_b} + \boldsymbol{F}_D + \boldsymbol{F}_{VM} \quad (1)$$

The first term on the right hand side is the relative buoyancy force (force divided by bubble mass). The other forces are drag and virtual mass force. The drag force is

$$\boldsymbol{F}_D = \frac{18\mu}{\rho_b d_b^2}\frac{C_D \mathrm{Re}}{24}(\boldsymbol{u}_b - \boldsymbol{u}) \quad (2)$$

where C_D is the drag coefficient, Re is the Reynolds number, ρ_b is the density of the bubble gas and d_b is the bubble diameter. The driving mechanism of the drag force is the velocity difference between the bubbles and the liquid $\boldsymbol{u}_b - \boldsymbol{u}$. Note that $\boldsymbol{u}$ is the instantaneous velocity of the background fluid

$$\boldsymbol{u} = \boldsymbol{U} + \acute{\boldsymbol{u}} \quad (3)$$

accounting for both the average velocity $\boldsymbol{U}$ and the turbulent fluctuations $\acute{\boldsymbol{u}}$. The turbulent fluctuations in the drag force cause turbulent dispersion. As in all models not resolving the turbulence, the turbulent dispersion is calculated by a sub-model. For Lagrangian tracking of bubbles (or particles) we apply a *random walk model* (Gosman & Ioannides, 1983) in which the turbulent velocity fluctuations are calculated by

$$\acute{\boldsymbol{u}} = \boldsymbol{\xi}\sqrt{k} \quad (4)$$

if a k-ϵ turbulence model is deployed. Here $\boldsymbol{\xi}$ is a random number. The time of which this velocity fluctuation is applied in the integration of the bubble trajectory is limited by the eddy lifetime (or the time it takes for a bubble to traverse through a turbulent eddy). The eddy lifetime is

$$\tau = 0.15\frac{k}{\epsilon} \quad (5)$$

for a k-ϵ model. The drag coefficient is provided by the expression of Tomiyama *et al.* (1998) for contaminated conditions with a correction for bubble interactions at higher volume fractions based on Tsuji *et al.* (1982).

Virtual mass force also known as added mass force is the force added to a bubble because an accelerating body is deflecting some volume of the surrounding fluid as it moves through it. The force is given as

$$\boldsymbol{F}_{VM} = C_{VM}\frac{\rho}{\rho_b}\left(\frac{D\boldsymbol{u}}{Dt} - \frac{d\boldsymbol{u}_b}{dt}\right) \quad (6)$$

where $C_{VM} = 0.5$ is the virtual mass coefficient. Lift force is normally included in reactor modelling, but sensitivity studies show no effect of the lift force in the reactor being studied. This is due to the absence of walls close to the bubbles. In such scenarios the shear rate is relatively small and the lift force can be discarded (Olsen & Popescu, 2014).

The bubble size is assumed to be governed by turbulence break up and coalescence. A model accounting for this is incorporated in the framework (Cloete *et al.*, 2009). The bubble diameter depends upon turbulent dissipation, surface tension and volume fraction among others.

The motion of the bubbles is coupled to the flow of the background fluid. The background fluid is a liquid with a gas on top as illustrated in Figure 1. The bubbles are removed upon entering the gas phase. An Eulerian VOF method conserving mass and momentum through the Navier-Stokes equations is deployed to calculate the flow of the continuous background phases (Hirt & Nichols, 1981). The interface between the continuous liquid and gas phases are tracked by the GEO reconstruct scheme (Youngs, 1982). The coupling with the Lagrangian bubbles is achieved through a source term in the momentum equation accounting for bubble drag

$$\rho\frac{D\mathbf{U}}{Dt} = \rho\boldsymbol{g} - \nabla p + \nabla\cdot[\mu_{\mathrm{eff}}(\nabla\boldsymbol{U} + \nabla\boldsymbol{U}^T)] + F_b \quad (7)$$

where μ_{eff} is the effective viscosity (molecular + turbulent) and F_b is the source term due to drag of bubbles. Turbulence and turbulent viscosity are quantified by the standard k-ϵ model (Launder & Spalding, 1974).

The modelling concept is implemented in ANSYS/Fluent 14.0. The PISO scheme is applied for pressure-velocity coupling, spatial discretization is second order or higher and the time discretization is implicit first order. The PISO scheme is normally robust with fast convergence.

VALIDATION EXPERIMENT

A series of validation experiments were performed in a 800 x 500 x 50 mm vessel as seen in Figure 1 in the introduction. Water was filled up to a depth of 500 mm leaving 300 mm clearance on top. Gas was injected through a lance as illustrated. Gas rates and lance position was varied. Two nozzles were applied in the experiments. Mostly a nozzle with two holes pointing outwards in the horizontal plane was applied. For one of the experimental runs, a nozzle with a single hole pointing downwards was applied. All nozzle holes had a diameter of d=2mm.

Water velocities were measured with Laser Doppler Velocimetry (LDV) at an array of predefined positions. The laser was focused such that the velocities were sampled at the centre plane. The reported velocity values are an average of 3 repetitions. Mixing characteristics were studied by adding a tracer on the side at the water surface. The dilution of the tracer can be seen as a measure of mixing efficiency. This part of the experiment was videotaped. A panel of 7 persons independently evaluated how long time it took for the tracer to be evenly distributed in the vessel. An average experimental mixing time was calculated based on this.

Case	Position	Δx mm	Δy mm	Gas rate ltr/min	Nozzle
1	1	300	250	2.5	2 horiz.
2	1	300	250	5.0	2 horiz.
3	1	300	250	7.5	2 horiz.
4	2 (up)	300	350	5.0	2 horiz.
5	3 (down)	300	150	5.0	2 horiz.
6	4 (out)	350	250	5.0	2 horiz.
7	1	300	250	5.0	1 vertical

Table 1: Experimental settings

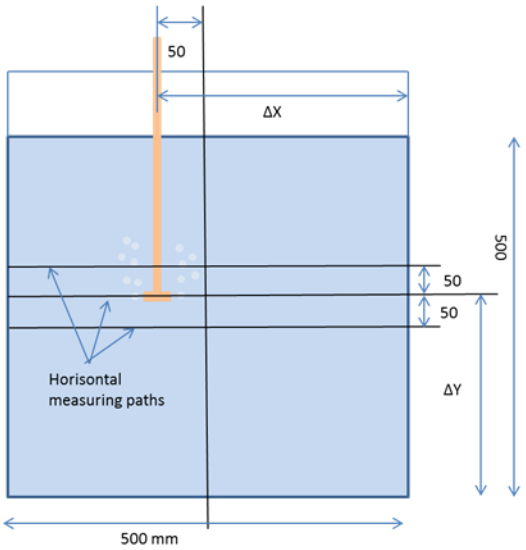

Figure 2: Measuring paths and lance positioning. The example show Δx=300mm.

The experimental matrix is shown in Table 1 and in the definition of lance and nozzle position is seen in Figure 2. A run was performed by positioning the lance, choosing the nozzle and adjusting the gas rate according to the given case in Table 1. During the experiments it was observed that the gas bubbles initially ascend fairly straight to the surface. However, after a while the circulation in the water interacts with the bubble plume making it incline towards the side. Thus measurements were recorded after this quasi steady state was established.

RESULTS

Following a grid dependence study, mathematical simulations were performed on the same cases as studied experimentally and defined by Table 1. Figure 1 shows a typical bubble field (here Case 2 is used as an example) where the bubbles rise to the free surface with a slight bend to the left. Figure 3 shows a typical flow field exposed to the same conditions as the bubble field. A strong upward stream from the gas injection point is seen. This is due to the buoyancy of the injected gas bubbles. This sets up a circulation in the liquid as demonstrated by the figure. This circulation interacts with the bubble plume, making it bend to the side after some time.

The velocity profiles for the different cases defined in Table 1 were extracted and compared to velocity profiles generated by mathematical simulations based on the modelling concept described above. The comparison of vertical and horizontal velocity components is seen in Figure 4 to Figure 7 for cases 1 and 2. Both cases have the same positioning of the lance and gas injection. The gas rate is varying. We see that the results from the modelling concept are consistent with the measurements: there is in fact very good agreement between the measured and calculated velocity profiles, which is encouraging. Other cases show similar consistency between experiments and model. We see from these profiles that the velocities increase with increasing gas rates. This is as expected.

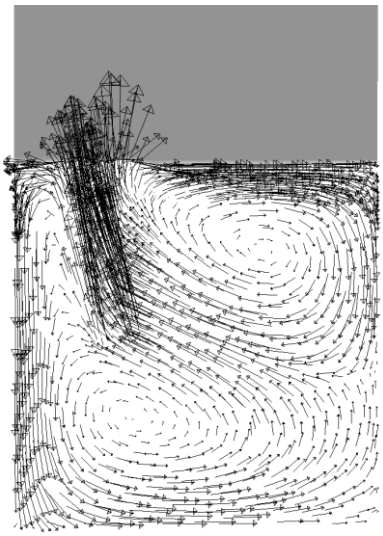

Figure 3: Typical velocity field.

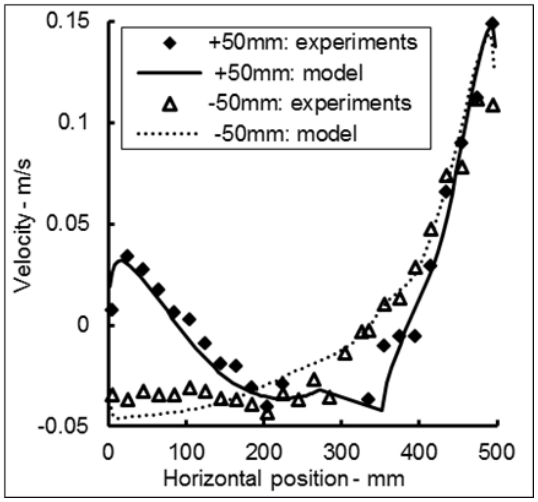

Figure 4: Profiles of vertical velocity for case 1 (2.5 ltr/min) at heights 50mm above and below vessel centre.

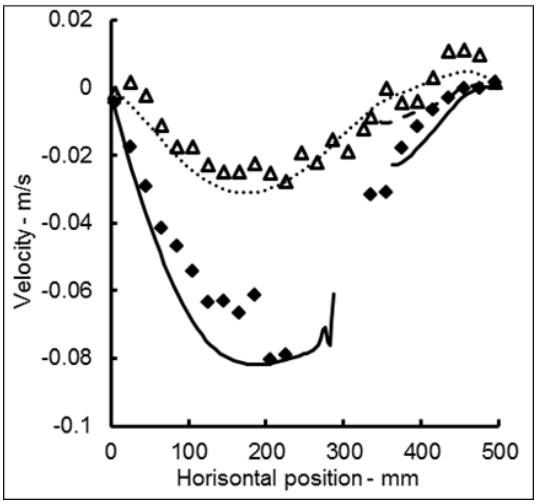

Figure 5: Profiles of horizontal velocity for case 1 (2.5 l/min) at heights 50 mm above and below vessel centre.

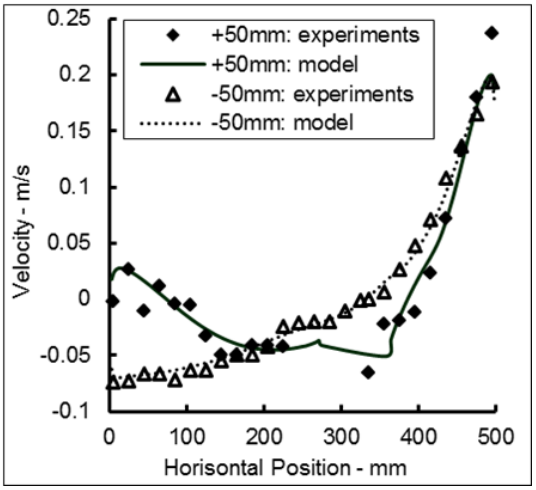

Figure 6: Profiles of vertical velocity for case 2 (5.0 l/min) at heights 50mm above and below vessel centre.

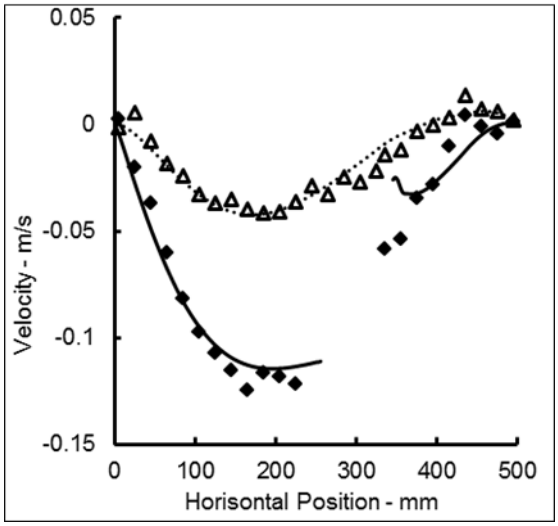

Figure 7: Profiles of horizontal velocity for case 2 (5.0 l/min) at heights 50mm above and below vessel centre.

Figure 8: Evolution of tracer concentration in Case 2 for experiment (left) and simulation (right) 11 seconds after tracer injection

The mixing characteristics were studied by adding a tracer in the water vessel after a quasi-steady flow field was established. The tracer follows the typical flow field and is mixed due to convection. In Figure 8 we see the tracer concentration 11 seconds after tracer injection for both the experiments and the computation. Considering that the tracer is continuously being added for 30 seconds in the experiment and dumped in all at once in the simulations, the tracer concentrations are quite comparable for the experiments and mathematical model.

The mixing time in the mathematical simulations was extracted based on the evolution of a normalized tracer concentration. The difference between the maximum and average concentration in the centre plane was divided by the average concentration to define the normalized concentration. This is seen in Figure 9 where also a target concentration is plotted. The target concentration was decided based on tuning the computational and experimental mixing time for Case 2. With a target defined, the mixing time for the mathematical simulations was extracted. A comparison of the experimental and mathematical mixing times is seen in Figure 10 and Figure 11 for cases 1 to 5.

.

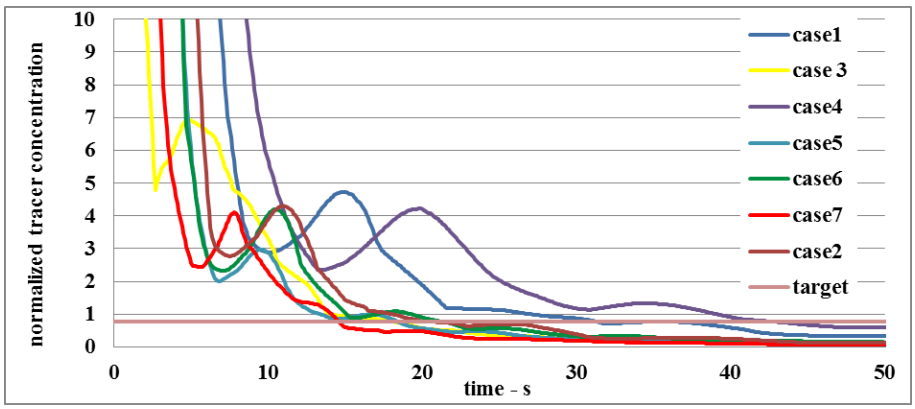

Figure 9: Normalized tracer concentration as function of time for all cases.

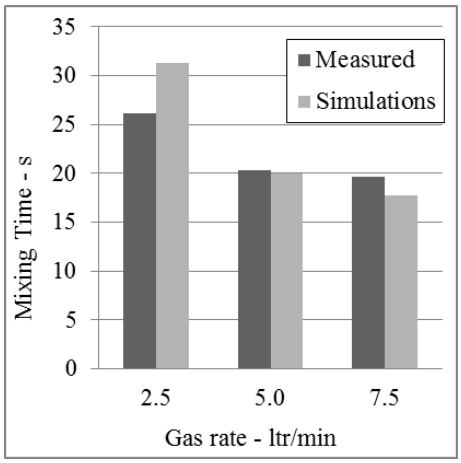

Figure 10: Mixing time and gas rate.

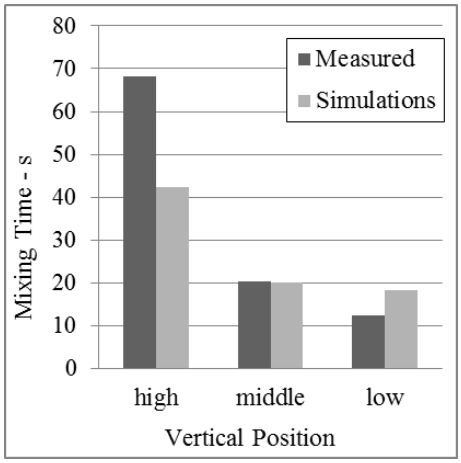

Figure 11: Mixing time and horizontal position of gas injection.

Mixing time estimated by mathematical simulations compare reasonably well with the mixing times obtained from the experiments. In Figure 10 we see that mixing speeds up with increasing gas rates. This is predicted both by the experiments and the simulations. Quantitatively there are some discrepancies, but this might be explained by the tracer being continuously added for 30 seconds in the experiment while dumped in all at once in the simulations, or the manual methodology of extracting the experimental mixing times. Still the experimental and computational mixing times are reasonably close.

In Figure 11 we see how mixing is improved as we lower the lance deeper into the vessel. This is confirmed both experimentally and mathematically. Efficient mixing is normally only achieved above the gas injection point. Below this point the flow and convection is weaker. Thus mixing improves when the lance is moved closer to the bottom of the vessel.

CONCLUSION

A mathematical model for simulations of the hydrodynamic behaviour of a bubble driven reactor has been developed. The model has previously been verified against experimental data from reactors with bottom blowing of gas. Here it was tested against experiments with gas injection from a submerged lance.

A series of experiments were performed on lance stirred reactors in an air-water system. Liquid velocities were measured and mixing characteristics documented by adding a tracer. The model was compared against these experiments, and shown to be quite consistent with the experimental results.

It was shown that mixing improves with increasing gas rates, and by lowering the point of gas injection. This is as expected. The modelling concept can thus be applied to study reactor design and operations provided that material properties and reaction dynamics (mass transfer descriptions) are implemented.

ACKNOWLEDGEMENT

This study was conducted in the GasReSi-project funded by the Norwegian Research Council and Elkem.

REFERENCES

CLOETE, S., OLSEN, J.E., & SKJETNE, P. (2009). "CFD modeling of plume and free surface behavior resulting from a sub-sea gas release". *Applied Ocean Research*, **31**(3), 220-225.

GOSMAN, A.D., & IOANNIDES, E. (1983). "Aspects of computer simulation of liquid-fuelled combustors". *J.Energy*, **7**, 482-490.

HIRT, C.W., & NICHOLS, B.D. (1981). "Volume of fluid (VOF) method for the dynamics of free boundaries". *Journal of Computational Physics*, **39**(1), 201-225.

LAUNDER, B.E., & SPALDING, D. (1974). "The numerical computation of turbulent flows". *Computer methods in applied mechanics and engineering*, **3**, 269-289.

OLSEN, J.E., & CLOETE, S. (2009). "Coupled DPM and VOF model for analyses of gas stirred ladles at higher gas rates". *Proc. of the Seventh International Conference on CFD in the Minerals and Process Industries*, Melbourne.

OLSEN, J.E., & POPESCU, M. (2014). "On the effect of lift forces in bubble plumes". *Progress in Computational Fluid Dynamics*, **5**.

TOMIYAMA, A., KATAOKA, I., ZUN, I., & SAKAGUCHI, T. (1998). "Drag coeffcients of single bubbles under normal and micro gravity conditions". *JSME International Journal, Series B*, **41**, 472-479.

TSUJI, Y., MORIKAWA, Y., & TERASHIMA, K. (1982). "Fluid-dynamic interaction between two spheres". *Int.J.Multiphase Flow*, **8**(1), 71-82.

YOUNGS, D.L. (1982). Time-Dependent Multi-Material Flow with Large Fluid Distortion. In K. W. Morton & M. J. Banes (Eds.), *Numerical Methods for Fluid Dynamics*: Academic Press.

